1 Role of the South Pacific Convergence Zone in West Antarctic Decadal Climate Variability 2 Kyle R. Clem<sup>1</sup>, Benjamin R. Lintner<sup>1,2</sup>, Anthony J. Broccoli<sup>1,2</sup>, and James R. Miller<sup>1,3</sup> 3 4 <sup>1</sup> Institute of Earth, Ocean, and Atmospheric Sciences, Rutgers, The State University of New 5 Jersey, New Brunswick, New Jersey 6 <sup>2</sup> Department of Environmental Sciences, Rutgers, The State University of New Jersey, New 7 8 Brunswick, New Jersey <sup>3</sup> Department of Marine and Coastal Sciences, Rutgers, The State University of New Jersey, New 9 10 Brunswick, New Jersey 11 12 Submitted to *Geophysical Research Letters* 13 January 2019 14 Revised March 2019 Revised May 2019 15 16 Corresponding author address: Kyle R. Clem, Institute of Earth, Ocean, and Atmospheric 17 Sciences, Environmental & Natural Resource Sciences Building, 14 College Farm Road, New 18 Brunswick, New Jersey, 08901, kyle.clem@rutgers.edu. 19 20 Main Point #1: Decadal variability in SST and precipitation along the SPCZ's poleward edge is 21 22 coherent with the Interdecadal Pacific Oscillation (IPO). 23 24 Main Point #2: The IPO influence on West Antarctic climate is in part tied to a SPCZ 25 teleconnection to the Amundsen Sea Low (ASL). 26 Main Point #3: Enhanced rainfall in the SPCZ, consistent with negative IPO, cools the Antarctic 27 Peninsula and warms the Ross Ice Shelf and East Antarctica. 28 29 30

## **Abstract**

Regional atmospheric circulation along coastal West Antarctica associated with the Amundsen Sea Low (ASL) mediates ice shelf melt that governs Antarctica's contribution to global sea level rise. In this study, the South Pacific Convergence Zone (SPCZ) is identified as a significant driver of ASL variability on decadal time scales. Using the Community Earth System Model, we impose a positive sea surface temperature anomaly in the SPCZ that reproduces an increase in convective rainfall in the southwest SPCZ that has been observed in recent decades, consistent with the Interdecadal Pacific Oscillation (IPO). Many of the major observed climate shifts across West Antarctica during the 2000-2014 period when the IPO was in its negative phase can be explained via a teleconnection over the ASL emanating from the SPCZ. Knowledge of these relationships significantly enhances our understanding and interpretation of past and future West Antarctic climate variability.

# **Plain Language Summary**

Deep convective rainfall in the South Pacific Convergence Zone (SPCZ) alters the regional atmospheric circulation along coastal West Antarctica impacting the regional climate and potentially driving warm ocean water upwelling that melts ice shelves. Increases in SPCZ rainfall cause cooling on the Antarctic Peninsula and warming across the Ross Ice Shelf and portions of East Antarctica. Such conditions were observed during the 2000-2014 period in which the phase of the Interdecadal Pacific Oscillation (IPO), a naturally-occurring mode of tropical Pacific decadal variability, was negative. The influence of the SPCZ on West Antarctic climate is consistent with observed shifts in West Antarctic climate over the period 2000-2014. Therefore, the SPCZ, though a tropical climate feature, is found to be an important driver of West Antarctic climate on decadal time scales governed by the IPO.

### 1. Introduction

56

57

58

59

60

61

62

63

64

65

66

67

68

69

70

71

72

73

74

75

76

77

78

West Antarctica is losing mass and contributing to global sea level rise at an increasing rate (The IMBIE team, 2018) with the potential to contribute up to one meter of global sea level rise by the end of this century (DeConto & Pollard, 2016). Recent mass loss is primarily tied to basal melting and subsequent thinning of floating ice shelves due to influxes of warm circumpolar deep water onto the continental shelf (Dutrieux et al., 2014; Pritchard et al., 2012; Shepherd et al., 2004; Thoma et al., 2008). Melting of ice shelves from below (via basal melting) and at the surface (via warming air temperatures; as seen on the Antarctic Peninsula and Ross Ice Shelf (Fahnestock et al., 2002; Nicolas et al., 2017)) is tied to regional atmospheric circulation in the Amundsen Sea region. This controls local zonal winds over the continental shelf break that mediates basal melt via Ekman transport (Dutrieux et al., 2014; Jenkins et al., 2010; Steig et al., 2012; Turner et al., 2017), and surface melt through thermal advection and radiative warming (Clem et al., 2018; Nicolas et al., 2017; Trusel et al., 2013, 2015). While recent studies have pointed to tropical variability modulating the atmospheric circulation and surface climate of West Antarctica, they have yet to identify a consistent mechanism explaining the marked seasonality of recent decadal climate trends (Jones et al., 2016; Turner et al., 2016). In particular, studies have offered competing hypotheses while often focusing on either localized regions of Antarctica or individual seasons that may not address, or may even contradict, observed climate changes in other regions or seasons. Reconciling the findings of recent studies and improving knowledge of decadal processes in this region will aid in understanding past and future West Antarctic climate variability on decadal time scales. Current understanding of how tropical variability influences West Antarctic climate varies by season and by tropical basin (Yuan et al., 2018), obscuring individual signals that could be used for future predictions. Several studies have demonstrated that the El Niño Southern Oscillation (ENSO) significantly influences West Antarctic climate and ice sheet mass balance by forcing interannual changes in the position and intensity of the Amundsen Sea Low (ASL) (Clem et al., 2017; Deb et al., 2018; Fogt et al., 2012; Hosking et al., 2013; Paolo et al., 2018; Raphael et al., 2016). More recent studies have emphasized that low frequency tropical variability, namely the Pacific Decadal Oscillation (PDO) / Interdecadal Pacific Oscillation (IPO) (Clem & Fogt, 2015; Meehl et al., 2016; Purich et al., 2016) and the Atlantic Multidecadal Oscillation (Li et al., 2014), may also affect West Antarctic climate on decadal time scales. Certainly, more detailed knowledge of how naturally occurring modes of tropical variability influence West Antarctica would enhance understanding and interpretation of past and future climate change in this region, potentially enhancing predictive capacity of future West Antarctic climate and mass balance.

(Clem & Fogt, 2015) first documented a linear relationship between a negative trend in the PDO (similar to the IPO) and warming of West Antarctica during the spring season, but their study was limited to a single season in which the PDO signal was obscured by concurrent La Niña conditions. (Clem & Renwick, 2015; Schneider et al., 2012) showed that spring warming of West Antarctica was correlated with convection in the SPCZ, but these studies did not explore the Rossby wave mechanism underlying this relationship or whether the SPCZ is tied to climatic changes seen in other seasons.

Other studies have used idealized climate model experiments to explore the IPO teleconnection to Antarctica. (Trenberth et al., 2014; Meehl et al., 2016) showed that a cold convective anomaly in the central equatorial Pacific associated with the IPO negative phase caused deepening of the ASL that was consistent with West Antarctic warming as well as sea ice

increase in the Ross Sea. However, the (negative) heating anomaly applied in these studies lies within the Niño 3.4 region, thus, it is not possible to distinguish this teleconnection from that of La Niña. Furthermore, (Turner et al., 2016) recently showed that over 1999-2014, when the IPO was negative, the Antarctic Peninsula cooled, and (Clem et al., 2018) showed the negative IPO was associated with warming on the Ross Ice Shelf. These post-1999 climate trends mark a sharp reversal of the warming (cooling) that was observed on the Antarctic Peninsula (Ross Ice Shelf) prior to 1999 (see Fig. 1). Moreover, they are not fully consistent with ASL deepening as suggested by (Meehl et al., 2016; Trenberth et al., 2014). Turner et al. (2016) attributed Antarctic Peninsula cooling to increased cyclonic activity in Drake Passage. However, they note that in summer when Antarctic Peninsula cooling is strongest, the tropical teleconnection is weak because of unfavorable conditions for Rossby wave propagation into high latitudes (Jin & Kirtman, 2009; Scott Yiu & Maycock, 2019). Therefore, while prior studies implicate the IPO as an important driver of West Antarctic decadal climate variability, no consistent explanation links the recent negative IPO event to the sharp reversal in West Antarctic climate trends observed during the same period. Thus, the full impact of the IPO on West Antarctic climate is uncertain. This study re-examines the IPO teleconnection to West Antarctica by focusing on the role of the SPCZ.

119

120

121

122

123

124

102

103

104

105

106

107

108

109

110

111

112

113

114

115

116

117

118

### 2. Data Sets, Model, and Methods

A map of the study area is provided in Figure 1. Station temperature data are from the Antarctic READER project (Turner et al., 2004); annual-mean normalized temperature anomalies from the 1979-2014 climatology are averaged across five Antarctic Peninsula stations: Rothera, Vernadsky, Bellingshausen, Esperanza, and Marambio. Sea ice concentrations around

the Antarctic Peninsula are from the Hadley Centre Sea Ice and SST dataset (Rayner et al., 2003). Central West Antarctic temperatures are obtained from the reconstructed Byrd station record of (Bromwich et al., 2012). Several fields from the European Centre for Medium-Range Weather Forecasts-Interim reanalysis (ERA-Interim) (Dee et al., 2011), including 2m temperatures over the Ross Ice Shelf, tropical precipitation, and upper-tropospheric winds, are analyzed.

Sea surface temperatures (SSTs) are from the National Oceanic and Atmospheric Administration (NOAA) Extended Reconstructed SST version 4 (ERSSTV4) (Huang et al., 2015, 2016; Liu et al., 2015). The IPO index is taken from the tripole index (Henley et al., 2015) provided by NOAA's Physical Sciences Division.

To test if SST and precipitation anomalies in the SPCZ affect the climate of West Antarctica, we perform two experiments using the NCAR Community Earth System Model version 1.2 (CESM1.2) (Hurrell et al., 2013). The model was run in atmosphere-only mode using CAM5 physics and dynamics at a horizontal resolution of 1.9°x2.5° latitude-longitude. We use pre-industrial concentrations of greenhouse gases and prescribe climatological sea ice concentrations and SSTs: the sea ice climatology spans 1982-2001 and the SST climatology spans 1950-2017. We perform two 30-year simulations following a one-year spin-up: one control run with annually repeating climatological SSTs, and one perturbed run with a +2°C SST anomaly in the southwest SPCZ region 160-175°E, 15-25°S imposed on the same climatological SSTs as in the control run. The SST anomaly is linearly dampened to zero following the sine of the change in latitude/longitude moving away from the box.

We employ a linear least squares technique for trend and regression analysis. Statistical significance of trends and regressions is assessed following a Student's two-tailed *t* test.

Climatological monthly differences between the two 30-year simulations are investigated and statistical significance of these differences is assessed using a Student's two-tailed *t* test with 58 (n-2) degrees of freedom.

### 3. Results

The reversal in West Antarctic climate trends coinciding with the IPO transition to its negative phase at the end of the 20<sup>th</sup> century is illustrated in Figure 1. After 1999, there is a weak Antarctic Peninsula cooling trend along with an increase in sea ice, as noted by (Turner et al., 2016), marking a dramatic shift from what was the most rapidly warming region on the planet from the 1950s to 1990s (Vaughan, 2001). Over the continental interior, the strong warming at Byrd station (Bromwich et al., 2012) also stopped after 1999 with weak cooling thereafter.

Farther west over the Ross Ice Shelf, a trend reversal from cooling to warming occurred after 1999. This pattern reflects a dipole in temperature anomalies between the Peninsula and Ross Ice Shelf, which is characteristic of ASL weakening (Clem et al., 2017; Yuan & Martinson, 2001). This study is motivated by the fact that cooling on the Antarctic Peninsula and at Byrd station and warming over the Ross Ice Shelf are not fully explained by ASL deepening associated with equatorial Pacific cooling (Meehl et al., 2016; Trenberth et al., 2014).

Figure 1c-e shows that the negative IPO transition, captured by the 1979-2014 trend, was associated with significant ocean warming and increases in rainfall along the poleward edge of the SPCZ. SSTs in the southwest SPCZ, which correlate with the IPO at 0.75 (p<0.001), experienced a nearly stepwise transition to predominantly positive anomalies after the late 1990s (Fig. 1c). This ocean warming has resulted in an increase in SPCZ rainfall (Fig. 1e). This relationship is consistent with previous work demonstrating the IPO's significant influence on

SST and precipitation variability along the southwest/poleward edge of the SPCZ (e.g. Folland, 2002). Supplementary Fig. 1 confirms that while ENSO variability influences SST and precipitation variability in the SPCZ's equatorial portion, the IPO dominates along its poleward edge.

We hypothesize that increased deep convection in the SPCZ may be an important component of the IPO teleconnection to West Antarctica. To investigate this hypothesis, we perform a sensitivity experiment with an imposed +2°C SST anomaly along the SPCZ's southwestern edge (160-175°E, 15-25°S; black box in Fig. 1d-e); note the SPCZ is denoted by the 4 mm day<sup>-1</sup> climatological isohyet (bold black line in Fig. 1d-e). We intentionally position the SST anomaly partially outside of the 4 mm day<sup>-1</sup> line to ensure that the convective response is confined to the poleward edge of the SPCZ, as seen in the observed trend and consistent with where previous studies (e.g. (Clem & Renwick, 2015)) found a strong teleconnection to the ASL region. We investigate 30-year climatological monthly differences between the perturbed simulation and control simulations: the only difference between these simulations is the SPCZ region SST anomaly.

The SST anomaly produces increased precipitation in the SPCZ (Fig. S2) that aligns spatially with the observed precipitation trend over the period 1979-2014 (Fig. 1e). The simulated precipitation anomalies, of 5-12 mm day<sup>-1</sup>, lie within the range of observed precipitation anomalies in this region (up to 15mm day<sup>-1</sup>, not shown). While the 4mm day<sup>-1</sup> isohyet shifts poleward during the austral warm season and equatorward during the cold season, the SPCZ remains active during all seasons, and the imposed SST anomaly yields a convective precipitation anomaly and an anomalous Rossby wave source (RWS) south of the SPCZ in all four seasons (Fig. S2).

We suggest that the diagonal poleward extension of the SPCZ toward a strong climatological RWS situated south of the SPCZ is a key aspect of its capacity to modulate Antarctic climate. Here, strong upper-tropospheric vorticity gradients along the sub-tropical jet stream (and divergence in the exit region of the sub-tropical jet) coincide with deep ascent within the SPCZ producing a strong RWS that is maintained year-round, unlike the central tropical Pacific where the RWS is largely absent in the austral warm season (e.g. (Jin & Kirtman, 2009)). The model reproduces the year-round RWS south of the SPCZ seen in ERA-Interim (Fig. S3). Therefore, the SPCZ is a potential hot spot for producing poleward-propagating Rossby waves in all seasons and may be an important component of the IPO teleconnection in West Antarctica.

Figure 2 depicts the SPCZ-forced circulation anomalies obtained by the leading empirical orthogonal function (EOF) of monthly 250 hPa geopotential height (Z250) anomalies (perturbed monthly climatology minus control monthly climatology). The imposed SST anomaly is indicated by the black hatching. The relationship with surface air temperature (SAT) is obtained by regressing the Z250 principal component (PC) time series onto the perturbed monthly SAT anomaly field. The raw monthly Z250 anomalies used to calculate the EOF are provided in Fig. S4.

The leading EOF, explaining 46.5% of the Z250 monthly variability, depicts a Rossby wave train emanating from the SPCZ with centers of action in the Ross-Amundsen Sea (150°W) and Drake Passage (60°W). The positive phase of this pattern occurs during the austral warm months (December-May, DJFMAM; Fig. 2c), which features an anomalous anticyclone in the Ross and Amundsen Seas and an anomalous cyclone over Drake Passage, the latter consistent with the circulation pattern that cooled the Antarctic Peninsula (Turner et al., 2016). This pattern emerges in December and peaks in amplitude during March and April. The circulation results in

warm northerly flow across the Ross Ice Shelf and portions of East Antarctica, and cold southerly flow across the Antarctic Peninsula and portions of continental West Antarctica. The temperature anomalies are consistent with the observed post-1999 climate trends. The negative phase of the circulation pattern occurs during the austral cold months (June-November, JJASON; Fig. 2c), first emerging in June, reaching its peak amplitude in July, and persisting through midspring. May and November mark transition months when the center of the circulation anomalies are located near nodes of the leading EOF. This points to a propagating pattern consistent with tropically-forced Rossby wave trains.

The seasonality of the circulation anomalies follows the seasonality of the background jet streams. Figure 2b shows the leading EOF of zonal wind anomalies at 300 hPa (U300; from the 30 year control run) poleward of 20°S; the monthly U300 PC is shown alongside the Z250 PC in Fig. 2c. The positive phase of the SPCZ pattern occurs during the austral warm months when the RWS is weakest / located farthest west but is compensated by seasonally strong tropical ascent (see Fig. S5 for monthly velocity potential anomalies). During winter and spring months the weaker tropical ascent is compensated by a stronger vorticity gradient along the sub-tropical jet. The background jet streams clearly contribute to determining the sign and location of the circulation anomalies, consistent with previous studies (e.g. (Dawson et al., 2011)). However, our results show that an anomalous Rossby wave train is established in all seasons owing to the close proximity of the SPCZ to a year-round RWS north of New Zealand. This occurs even during summer when the RWS is weak, which does not occur in the central and eastern equatorial Pacific during summer (Jin & Kirtman, 2009).

Next, we examine the circulation and climate impacts grouped into the extended warm and cold seasons, DFJMAM and JJASON, respectively (Fig. 3). During DJFMAM (Fig. 3a,c),

the SPCZ heating induces a strong anticyclone in the ASL region that produces, via thermal advection, cooling across the Antarctic Peninsula and Bellingshausen Sea and warming across the Ross Ice Shelf (consistent with the recent warming at McMurdo station located on the western Ross Ice Shelf (Ludescher et al., 2017)). In JJASON (Fig. 3b,d), the ASL is deepened west of its mean position in the northern Ross Sea and an anticyclone is located over the Bellingshausen Sea. The deepened ASL in the Ross Sea matches the observed September-November sea level pressure trend over 1979-2014 (Clem & Fogt, 2015; Clem & Renwick, 2015) and the pattern is consistent with Ross Ice Shelf warming and Antarctic Peninsula cooling.

#### 4. Discussion and Conclusions

This study shows that the SPCZ produces a teleconnection over the ASL region resulting in climate anomalies that are consistent with the observed post-1999 cooling on the Antarctic Peninsula and warming on the Ross Ice Shelf. During the austral warm months (DJFMAM), a Rossby wave train forced by anomalous diabatic heating in the SPCZ results in enhanced cyclonic activity north of Drake Passage that would produce cooling and increased sea ice on the Antarctic Peninsula. The predominant feature of the DJFMAM teleconnection is an anomalous anticyclone over the Amundsen Sea, which would further enhance cooling on the Peninsula and result in warming across the Ross Ice Shelf. There is an important difference between our results and (Turner et al., 2016) regarding the strength of the tropical teleconnection in summer. They find that the teleconnection is weak, whereas our results show that the SPCZ teleconnection in summer is surprisingly strong, most likely because of its favorable location to a RWS north of New Zealand. During the austral cold months (JJASON), the ASL is deepened over the Ross Sea with an anomalous anticyclone in the Bellingshausen Sea. This results in weak cooling on the

Peninsula, while the warming is shifted eastward toward central West Antarctica and the Amundsen Sea Embayment.

We note that the circulation pattern forced by the SPCZ in DJFMAM, specifically the anticyclone over the Amundsen Sea, has not been seen in observations. Figure 4 shows the SPCZ-forced circulation alongside the observed circulation change from ERA-Interim (an epoch of 1999-2014 minus 1979-1998) and a composite of four DJFMAM positive Southern Annular Mode (SAM) events that occurred due to internal variability in the SPCZ perturbation run (similar results are found using groups of five and six SAM events). We examine zonal anomalies (by subtracting the zonal mean) to better capture the tropically-forced component of the circulation.

During DJFMAM (Fig. 4c) ERA-Interim shows a slight deepening of the ASL, contrary to the anticyclone expected from the SPCZ. We suggest that the concurrent cooling in the equatorial Pacific (Meehl et al., 2016; Trenberth et al., 2014), combined with the positive trend in the SAM during DJFMAM over 1979-2014 due to ozone depletion and tropical forcing (Schneider et al., 2015; Thompson et al., 2011; Thompson & Solomon, 2002), may destructively interfere with the SPCZ teleconnection over the Amundsen Sea. As the SPCZ and equatorially-forced teleconnections cancel over the Amundsen Sea, the result is largely consistent with the positive SAM pattern (compare Fig. 4c and 4e).

The SPCZ wave train in JJASON matches the deepening of the ASL over the Ross Sea seen in ERA-Interim (compare Fig. 4b and 4d). However, the anticyclone over the Bellingshausen Sea is not seen and/or it is located farther west than observed. We infer that the anticyclone is largely canceled by the cooling in the equatorial Pacific as well as the increase in La Niña events in this season (Clem & Fogt, 2015; Meehl et al., 2016; Purich et al., 2016). This

is evidenced by a negligible Z250 trend in the Bellingshausen Sea (Fig. 4d) which is in stark contrast to what would be expected from equatorial Pacific cooling and increased La Niña conditions in this season. However, during the winter season (June-August), our results are consistent with (Ding et al., 2011) which identified an anticyclonic trend over the Amundsen Sea region.

Our results indicate that the IPO teleconnection to West Antarctica comprises two distinct and competing tropically-forced Rossby wave trains, one forced by the central equatorial Pacific and another by the SPCZ. Neither mechanism fully captures the observed circulation trends seen for 1999-2014, but when examined together the net response is highly consistent with the observed circulation changes and the post-1999 reversal in West Antarctic climate trends, including both the spatial and seasonal variability.

# Acknowledgements

K.R.C acknowledges support from a post-doctoral associate award from the Institute of Earth, Ocean, and Atmospheric Sciences at Rutgers, The State University of New Jersey. K.R.C. and B.R.L acknowledge support from NSF EAGER grant AGS-1842543. We thank Dr. Galen Collier of Rutgers's Office of Advanced Research Computing for his help porting CESM to the Rutgers Amarel Cluster. Antarctic weather station data can be accessed from the SCAR READER Project at <a href="https://legacy.bas.ac.uk/met/READER/">https://legacy.bas.ac.uk/met/READER/</a>. Reanalysis data from ERA-Interim can be accessed at <a href="https://apps.ecmwf.int/datasets/data/interim-full-daily/levtype=sfc/">https://apps.ecmwf.int/datasets/data/interim-full-daily/levtype=sfc/</a>.

## References

306

307 Bromwich, D. H., Nicolas, J. P., Monaghan, A. J., Lazzara, M. A., Keller, L. M., Weidner, G. A., & 308 Wilson, A. B. (2012). Central West Antarctica among the most rapidly warming regions 309 on Earth. *Nature Geoscience*, 6(2), 139–145. https://doi.org/10.1038/ngeo1671 310 Clem, K. R., & Fogt, R. L. (2015). South Pacific circulation changes and their connection to the 311 tropics and regional Antarctic warming in austral spring, 1979-2012: S. Pacific Trends 312 and Tropical Influence. Journal of Geophysical Research: Atmospheres, 120(7), 2773-313 2792. https://doi.org/10.1002/2014JD022940 314 Clem, K. R., & Renwick, J. A. (2015). Austral Spring Southern Hemisphere Circulation and 315 Temperature Changes and Links to the SPCZ. Journal of Climate, 28(18), 7371–7384. 316 https://doi.org/10.1175/JCLI-D-15-0125.1 317 Clem, K. R., Renwick, J. A., & McGregor, J. (2017). Large-Scale Forcing of the Amundsen Sea Low 318 and Its Influence on Sea Ice and West Antarctic Temperature. Journal of Climate, 30(20), 319 8405-8424. https://doi.org/10.1175/JCLI-D-16-0891.1 320 Clem, K. R., Orr, A., & Pope, J. O. (2018). The Springtime Influence of Natural Tropical Pacific 321 Variability on the Surface Climate of the Ross Ice Shelf, West Antarctica: Implications for Ice Shelf Thinning. Scientific Reports, 8(1). https://doi.org/10.1038/s41598-018-30496-5 322 Dawson, A., Matthews, A. J., & Stevens, D. P. (2011). Rossby wave dynamics of the North Pacific 323 324 extra-tropical response to El Niño: importance of the basic state in coupled GCMs. 325 Climate Dynamics, 37(1-2), 391-405. https://doi.org/10.1007/s00382-010-0854-7 326 Deb, P., Orr, A., Bromwich, D. H., Nicolas, J. P., Turner, J., & Hosking, J. S. (2018). Summer 327 Drivers of Atmospheric Variability Affecting Ice Shelf Thinning in the Amundsen Sea

| 328 | Embayment, West Antarctica. Geophysical Research Letters, 45(9), 4124–4133.                            |
|-----|--|
| 329 | https://doi.org/10.1029/2018GL077092   |
| 330 | DeConto, R. M., & Pollard, D. (2016). Contribution of Antarctica to past and future sea-level          |
| 331 | rise. Nature, 531(7596), 591–597. https://doi.org/10.1038/nature17145                                  |
| 332 | Dee, D. P., Uppala, S. M., Simmons, A. J., Berrisford, P., Poli, P., Kobayashi, S., et al. (2011). The |
| 333 | ERA-Interim reanalysis: configuration and performance of the data assimilation system.                 |
| 334 | Quarterly Journal of the Royal Meteorological Society, 137(656), 553–597.                              |
| 335 | https://doi.org/10.1002/qj.828   |
| 336 | Ding, Q., Steig, E. J., Battisti, D. S., & Küttel, M. (2011). Winter warming in West Antarctica        |
| 337 | caused by central tropical Pacific warming. Nature Geoscience, 4(6), 398–403.                          |
| 338 | https://doi.org/10.1038/ngeo1129   |
| 339 | Dutrieux, P., De Rydt, J., Jenkins, A., Holland, P. R., Ha, H. K., Lee, S. H., et al. (2014). Strong   |
| 340 | Sensitivity of Pine Island Ice-Shelf Melting to Climatic Variability. Science, 343(6167),              |
| 341 | 174–178. https://doi.org/10.1126/science.1244341   |
| 342 | Fahnestock, M. A., Abdalati, W., & Shuman, C. A. (2002). Long melt seasons on ice shelves of           |
| 343 | the Antarctic Peninsula: an analysis using satellite-based microwave emission                          |
| 344 | measurements. Annals of Glaciology, 34, 127–133.   |
| 345 | https://doi.org/10.3189/172756402781817798   |
| 346 | Fogt, R. L., Jones, J. M., & Renwick, J. (2012). Seasonal Zonal Asymmetries in the Southern            |
| 347 | Annular Mode and Their Impact on Regional Temperature Anomalies. Journal of                            |
| 348 | Climate, 25(18), 6253–6270. https://doi.org/10.1175/JCLI-D-11-00474.1                                  |

349 Folland, C. K. (2002). Relative influences of the Interdecadal Pacific Oscillation and ENSO on the 350 South Pacific Convergence Zone. *Geophysical Research Letters*, 29(13). 351 https://doi.org/10.1029/2001GL014201 352 Henley, B. J., Gergis, J., Karoly, D. J., Power, S., Kennedy, J., & Folland, C. K. (2015). A Tripole 353 Index for the Interdecadal Pacific Oscillation. Climate Dynamics, 45(11–12), 3077–3090. 354 https://doi.org/10.1007/s00382-015-2525-1 355 Hosking, J. S., Orr, A., Marshall, G. J., Turner, J., & Phillips, T. (2013). The Influence of the 356 Amundsen-Bellingshausen Seas Low on the Climate of West Antarctica and Its 357 Representation in Coupled Climate Model Simulations. Journal of Climate, 26(17), 6633-358 6648. https://doi.org/10.1175/JCLI-D-12-00813.1 359 Huang, B., Banzon, V. F., Freeman, E., Lawrimore, J., Liu, W., Peterson, T. C., et al. (2015). 360 Extended Reconstructed Sea Surface Temperature Version 4 (ERSST.v4). Part I: Upgrades 361 and Intercomparisons. Journal of Climate, 28(3), 911-930. https://doi.org/10.1175/JCLI-D-14-00006.1 362 363 Huang, B., Thorne, P. W., Smith, T. M., Liu, W., Lawrimore, J., Banzon, V. F., et al. (2016). 364 Further Exploring and Quantifying Uncertainties for Extended Reconstructed Sea Surface 365 Temperature (ERSST) Version 4 (v4). *Journal of Climate*, 29(9), 3119–3142. 366 https://doi.org/10.1175/JCLI-D-15-0430.1 367 Hurrell, J. W., Holland, M. M., Gent, P. R., Ghan, S., Kay, J. E., Kushner, P. J., et al. (2013). The 368 Community Earth System Model: A Framework for Collaborative Research. Bulletin of the American Meteorological Society, 94(9), 1339-1360. https://doi.org/10.1175/BAMS-369 D-12-00121.1 370

| 371 | Jenkins, A., Dutrieux, P., Jacobs, S. S., McPhail, S. D., Perrett, J. R., Webb, A. T., & White, D.    |
|-----|---|
| 372 | (2010). Observations beneath Pine Island Glacier in West Antarctica and implications for              |
| 373 | its retreat. Nature Geoscience, 3(7), 468–472. https://doi.org/10.1038/ngeo890                        |
| 374 | Jin, D., & Kirtman, B. P. (2009). Why the Southern Hemisphere ENSO responses lead ENSO.               |
| 375 | Journal of Geophysical Research, 114(D23). https://doi.org/10.1029/2009JD012657                       |
| 376 | Jones, J. M., Gille, S. T., Goosse, H., Abram, N. J., Canziani, P. O., Charman, D. J., et al. (2016). |
| 377 | Assessing recent trends in high-latitude Southern Hemisphere surface climate. Nature                  |
| 378 | Climate Change, 6(10), 917–926. https://doi.org/10.1038/nclimate3103                                  |
| 379 | Li, X., Holland, D. M., Gerber, E. P., & Yoo, C. (2014). Impacts of the north and tropical Atlantic   |
| 380 | Ocean on the Antarctic Peninsula and sea ice. <i>Nature</i> , 505(7484), 538–542.                     |
| 381 | https://doi.org/10.1038/nature12945   |
| 382 | Liu, W., Huang, B., Thorne, P. W., Banzon, V. F., Zhang, HM., Freeman, E., et al. (2015).             |
| 383 | Extended Reconstructed Sea Surface Temperature Version 4 (ERSST.v4): Part II.                         |
| 384 | Parametric and Structural Uncertainty Estimations. Journal of Climate, 28(3), 931–951.                |
| 385 | https://doi.org/10.1175/JCLI-D-14-00007.1   |
| 386 | Ludescher, J., Bunde, A., & Schellnhuber, H. J. (2017). Statistical significance of seasonal          |
| 387 | warming/cooling trends. Proceedings of the National Academy of Sciences, 114(15),                     |
| 388 | E2998–E3003. https://doi.org/10.1073/pnas.1700838114  |
| 389 | Meehl, G. A., Arblaster, J. M., Bitz, C. M., Chung, C. T. Y., & Teng, H. (2016). Antarctic sea-ice    |
| 390 | expansion between 2000 and 2014 driven by tropical Pacific decadal climate variability.               |
| 391 | Nature Geoscience, advance online publication. https://doi.org/10.1038/ngeo2751                       |

| 392 | Nicolas, J. P., Vogelmann, A. M., Scott, R. C., Wilson, A. B., Cadeddu, M. P., Bromwich, D. H., et    |
|-----|---|
| 393 | al. (2017). January 2016 extensive summer melt in West Antarctica favoured by strong El               |
| 394 | Niño. Nature Communications, 8, 15799. https://doi.org/10.1038/ncomms15799                            |
| 395 | Paolo, F. S., Padman, L., Fricker, H. A., Adusumilli, S., Howard, S., & Siegfried, M. R. (2018).      |
| 396 | Response of Pacific-sector Antarctic ice shelves to the El Niño/Southern Oscillation.                 |
| 397 | Nature Geoscience, 11(2), 121–126. https://doi.org/10.1038/s41561-017-0033-0                          |
| 398 | Pritchard, H. D., Ligtenberg, S. R. M., Fricker, H. A., Vaughan, D. G., van den Broeke, M. R., &      |
| 399 | Padman, L. (2012). Antarctic ice-sheet loss driven by basal melting of ice shelves.                   |
| 400 | Nature, 484(7395), 502–505. https://doi.org/10.1038/nature10968                                       |
| 401 | Purich, A., England, M. H., Cai, W., Chikamoto, Y., Timmermann, A., Fyfe, J. C., et al. (2016).       |
| 402 | Tropical Pacific SST Drivers of Recent Antarctic Sea Ice Trends. Journal of Climate,                  |
| 403 | 29(24), 8931–8948. https://doi.org/10.1175/JCLI-D-16-0440.1   |
| 404 | Raphael, M. N., Marshall, G. J., Turner, J., Fogt, R. L., Schneider, D., Dixon, D. A., et al. (2016). |
| 405 | The Amundsen Sea Low: Variability, Change, and Impact on Antarctic Climate. Bulletin of               |
| 406 | the American Meteorological Society, 97(1), 111–121. https://doi.org/10.1175/BAMS-D-                  |
| 407 | 14-00018.1  |
| 408 | Rayner, N. A., Parker, D. E., Horton, E. B., Folland, C. K., Alexander, L. V., Rowell, D. P., et al.  |
| 409 | (2003). Global analyses of sea surface temperature, sea ice, and night marine air                     |
| 410 | temperature since the late nineteenth century. Journal of Geophysical Research,                       |
| 411 | 108(D14). https://doi.org/10.1029/2002JD002670  |

| 412 | Schneider, D. P., Deser, C., & Okumura, Y. (2012). An assessment and interpretation of the           |
|-----|--|
| 413 | observed warming of West Antarctica in the austral spring. Climate Dynamics, 38(1–2),                |
| 414 | 323–347. https://doi.org/10.1007/s00382-010-0985-x   |
| 415 | Schneider, D. P., Deser, C., & Fan, T. (2015). Comparing the Impacts of Tropical SST Variability     |
| 416 | and Polar Stratospheric Ozone Loss on the Southern Ocean Westerly Winds. Journal of                  |
| 417 | Climate, 28(23), 9350–9372. https://doi.org/10.1175/JCLI-D-15-0090.1                                 |
| 418 | Scott Yiu, Y. Y., & Maycock, A. C. (2019). On the seasonality of the El Niño teleconnection to the   |
| 419 | Amundsen Sea region. Journal of Climate. https://doi.org/10.1175/JCLI-D-18-0813.1                    |
| 420 | Shepherd, A., Wingham, D., & Rignot, E. (2004). Warm ocean is eroding West Antarctic Ice             |
| 421 | Sheet: WARM OCEAN IS ERODING WAIS. Geophysical Research Letters, 31(23).                             |
| 422 | https://doi.org/10.1029/2004GL021106   |
| 423 | Steig, E. J., Ding, Q., Battisti, D. S., & Jenkins, A. (2012). Tropical forcing of Circumpolar Deep  |
| 424 | Water Inflow and outlet glacier thinning in the Amundsen Sea Embayment, West                         |
| 425 | Antarctica. Annals of Glaciology, 53(60), 19–28.   |
| 426 | https://doi.org/10.3189/2012AoG60A110  |
| 427 | The IMBIE team. (2018). Mass balance of the Antarctic Ice Sheet from 1992 to 2017. Nature,           |
| 428 | 558(7709), 219–222. https://doi.org/10.1038/s41586-018-0179-y  |
| 429 | Thoma, M., Jenkins, A., Holland, D., & Jacobs, S. (2008). Modelling Circumpolar Deep Water           |
| 430 | intrusions on the Amundsen Sea continental shelf, Antarctica. Geophysical Research                   |
| 431 | Letters, 35(18). https://doi.org/10.1029/2008GL034939  |
| 432 | Thompson, D. W. J., & Solomon, S. (2002). Interpretation of Recent Southern Hemisphere               |
| 433 | Climate Change. <i>Science</i> , <i>296</i> (5569), 895–899. https://doi.org/10.1126/science.1069270 |

| 434 | Thompson, D. W. J., Solomon, S., Kushner, P. J., England, M. H., Grise, K. M., & Karoly, D. J.             |
|-----|--|
| 435 | (2011). Signatures of the Antarctic ozone hole in Southern Hemisphere surface climate                      |
| 436 | change. Nature Geoscience, 4(11), 741–749. https://doi.org/10.1038/ngeo1296                                |
| 437 | Trenberth, K. E., Fasullo, J. T., Branstator, G., & Phillips, A. S. (2014). Seasonal aspects of the        |
| 438 | recent pause in surface warming. Nature Climate Change, 4(10), 911–916.                                    |
| 439 | https://doi.org/10.1038/nclimate2341   |
| 440 | Trusel, L. D., Frey, K. E., Das, S. B., Munneke, P. K., & van den Broeke, M. R. (2013). Satellite-         |
| 441 | based estimates of Antarctic surface meltwater fluxes: SATELLITE-BASED ANTARCTIC                           |
| 442 | MELT FLUXES. Geophysical Research Letters, 40(23), 6148–6153.  |
| 443 | https://doi.org/10.1002/2013GL058138   |
| 444 | Trusel, L. D., Frey, K. E., Das, S. B., Karnauskas, K. B., Kuipers Munneke, P., van Meijgaard, E., &       |
| 445 | van den Broeke, M. R. (2015). Divergent trajectories of Antarctic surface melt under two                   |
| 446 | twenty-first-century climate scenarios. Nature Geoscience, 8(12), 927–932.                                 |
| 447 | https://doi.org/10.1038/ngeo2563   |
| 448 | Turner, J., Colwell, S. R., Marshall, G. J., Lachlan-Cope, T. A., Carleton, A. M., Jones, P. D., et al.    |
| 449 | (2004). The SCAR READER project: Toward a high-quality database of mean Antarctic                          |
| 450 | meteorological observations. Journal of Climate, 17(14), 2890–2898.  |
| 451 | https://doi.org/10.1175/1520-0442(2004)017<2890:TSRPTA>2.0.CO;2  |
| 452 | Turner, John, Lu, H., White, I., King, J. C., Phillips, T., Hosking, J. S., et al. (2016). Absence of 21st |
| 453 | century warming on Antarctic Peninsula consistent with natural variability. Nature,                        |
| 454 | 535(7612), 411–415. https://doi.org/10.1038/nature18645  |

| 455 | Turner, John, Orr, A., Gudmundsson, G. H., Jenkins, A., Bingham, R. G., Hillenbrand, CD., &          |
|-----|--|
| 456 | Bracegirdle, T. J. (2017). Atmosphere-ocean-ice interactions in the Amundsen Sea                     |
| 457 | Embayment, West Antarctica: The Amundsen Sea Embayment, Antarctica. Reviews of                       |
| 458 | Geophysics, 55(1), 235–276. https://doi.org/10.1002/2016RG000532                                     |
| 459 | Vaughan, D. G. (2001). CLIMATE CHANGE: Devil in the Detail. Science, 293(5536), 1777–1779            |
| 460 | https://doi.org/10.1126/science.1065116  |
| 461 | Yuan, X., & Martinson, D. G. (2001). The Antarctic dipole and its predictability. <i>Geophysical</i> |
| 462 | Research Letters, 28(18), 3609–3612. https://doi.org/10.1029/2001GL012969                            |
| 463 | Yuan, X., Kaplan, M. R., & Cane, M. A. (2018). The Interconnected Global Climate System—A            |
| 464 | Review of Tropical–Polar Teleconnections. <i>Journal of Climate</i> , 31(15), 5765–5792.             |
| 465 | https://doi.org/10.1175/JCLI-D-16-0637.1   |
| 466 |  |
| 467 |  |

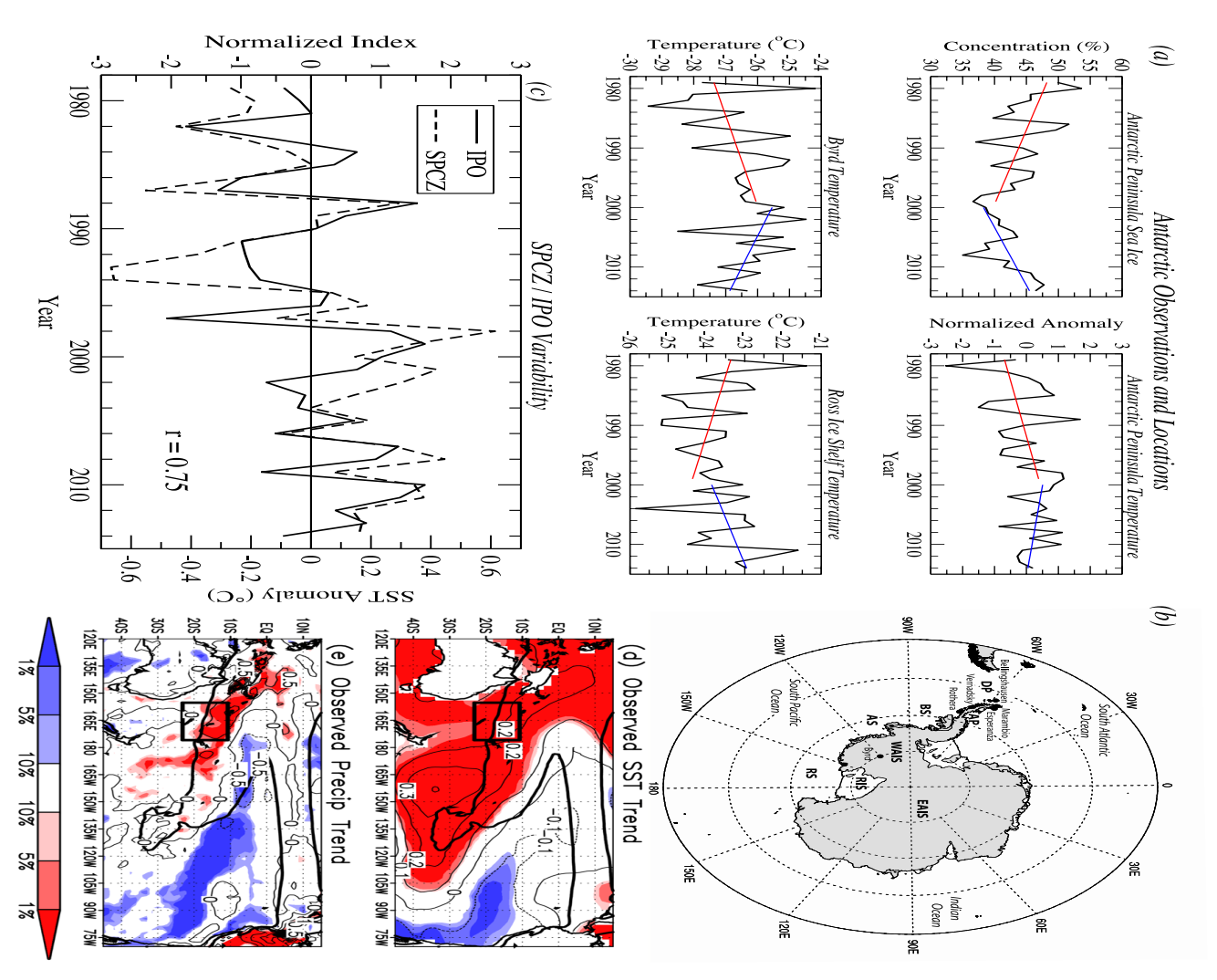


Figure 1. West Antarctic climate and SPCZ variability tied to low frequency tropical Pacific variability. (a) Annual-mean (January-December) time series of Antarctic Peninsula sea ice concentration averaged over 90-46°W, 60-72°S, normalized surface air temperature (SAT) anomalies averaged over five Antarctic Peninsula stations: Rothera, Vernadsky, Bellingshausen, Esperanza, and Marambio, Byrd station SAT (Bromwich et al., 2012), and Ross Ice Shelf SAT from ERA-Interim averaged over 160°E-156°W, and (b) map showing the study area and stations used for analysis: AP, Antarctic Peninsula; WAIS, West Antarctic Ice Sheet; RIS, Ross Ice Shelf; EAIS, East Antarctic Ice Sheet; DP, Drake Passage; BS, Bellingshausen Sea; AS, Amundsen Sea; RS, Ross Sea. (c) Annual-mean (May-April) time series of normalized IPO index (multiplied by -1 for visual comparison) and annual-mean SST anomalies in the southwest SPCZ (15-25°S, 160-175°E, region denoted by black box in (d-e)). (d-e) Observed annual-mean (May-April) linear trend (thin contours) of (d) ERSSTV4 tropical SST (°C decade<sup>-1</sup>) and (e) ERA-Interim tropical precipitation (mm day<sup>-1</sup> decade<sup>-1</sup>) over 1979-2014 capturing the IPO transition from positive to negative phase around 1999. Statistical significance of linear trends in (d-e) is shaded (reference color bar at bottom). Also given in (a) is the linear trend line in climate parameter over 1979-1999 (red) and 2000-2014 (blue), and in (d-e) the thick black line is the 4

469

470

471 472

473

474

475

476

477 478

479

480

481

482

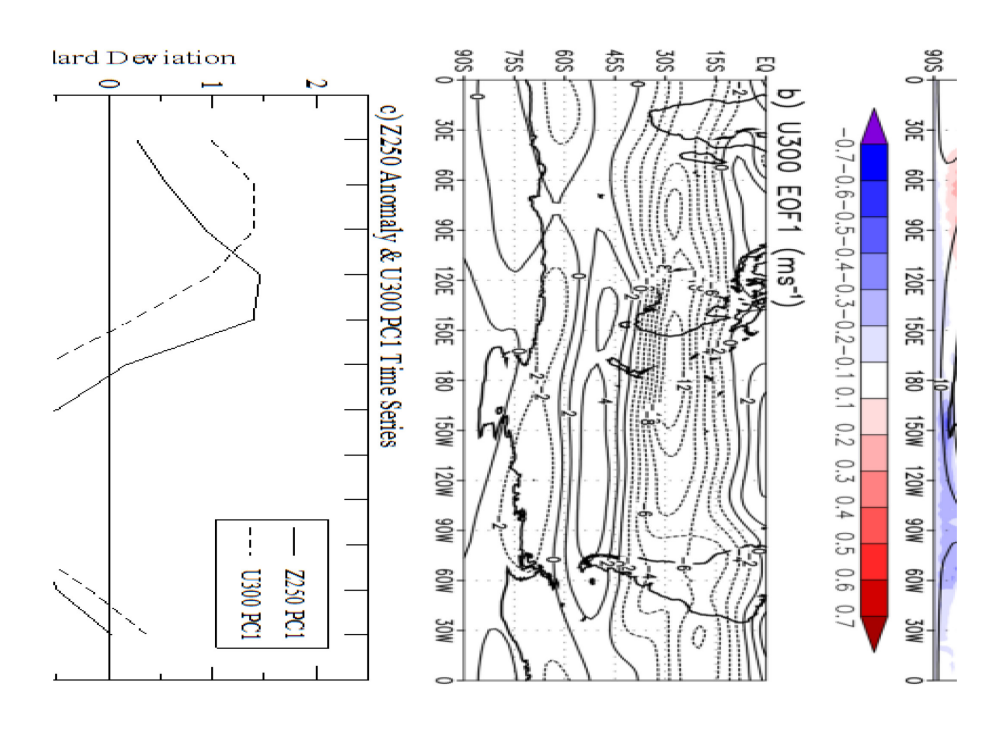


**Figure 2. Principal pattern of the SPCZ teleconnection and relationship with the Southern Hemisphere jet streams.** (a) EOF1 (explaining 46.5% of the variance) of monthly Z250 anomalies from SPCZ perturbation experiment (perturbed minus control) over the South Pacific (contours; m per standard deviation) and regression of Z250 PC1 onto SAT (shading; °C per standard deviation, reference color bar at bottom of (a)). The black hatched box indicates the location of the imposed SST anomaly. (b) EOF1 of monthly U300 winds over the Southern Hemisphere poleward of 20°S in the control experiment (contours; ms<sup>-1</sup> per standard deviation). (c) The normalized PC time series of Z250 perturbation anomalies and U300 anomalies EOF patterns in (a) and (b).

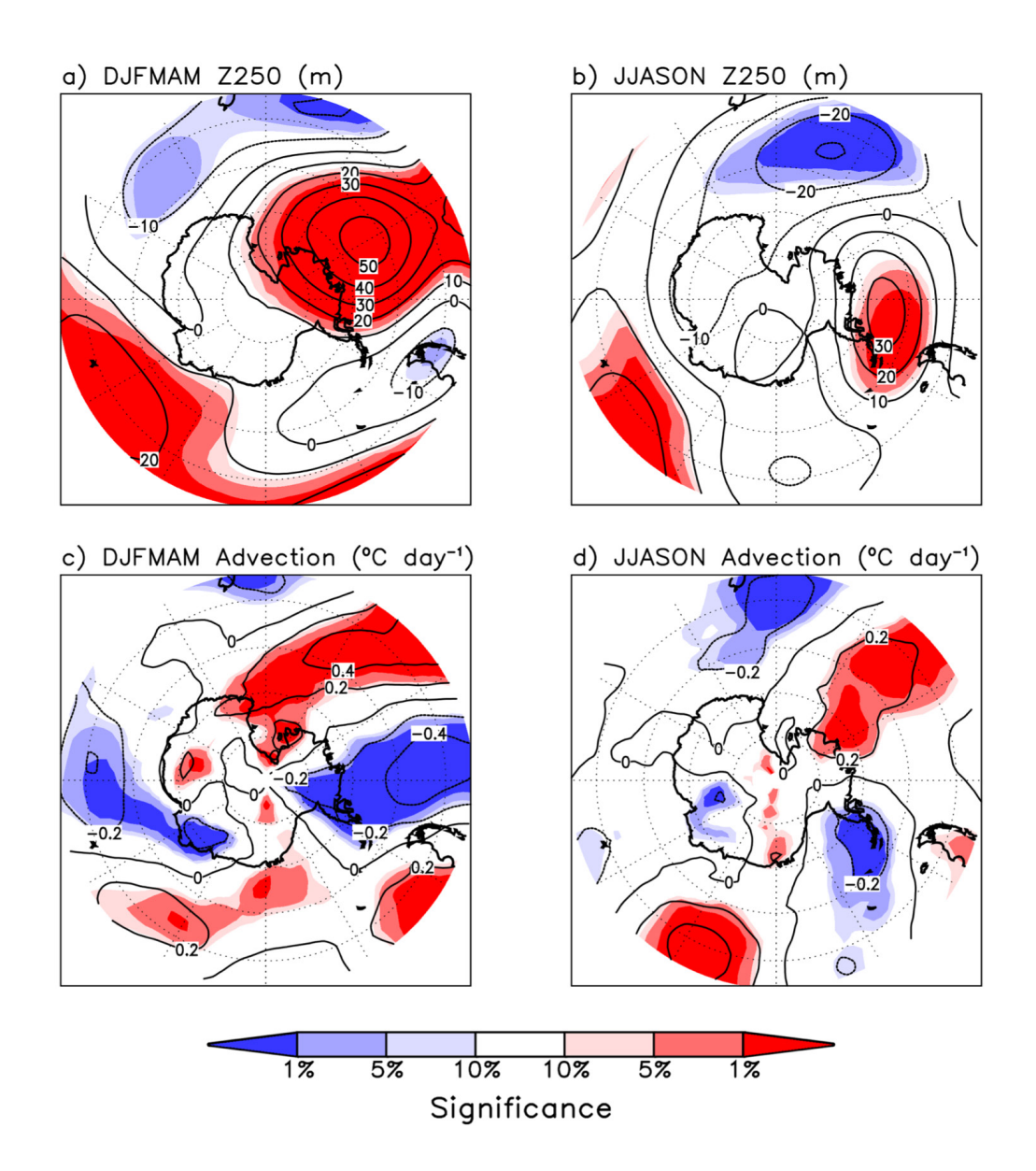
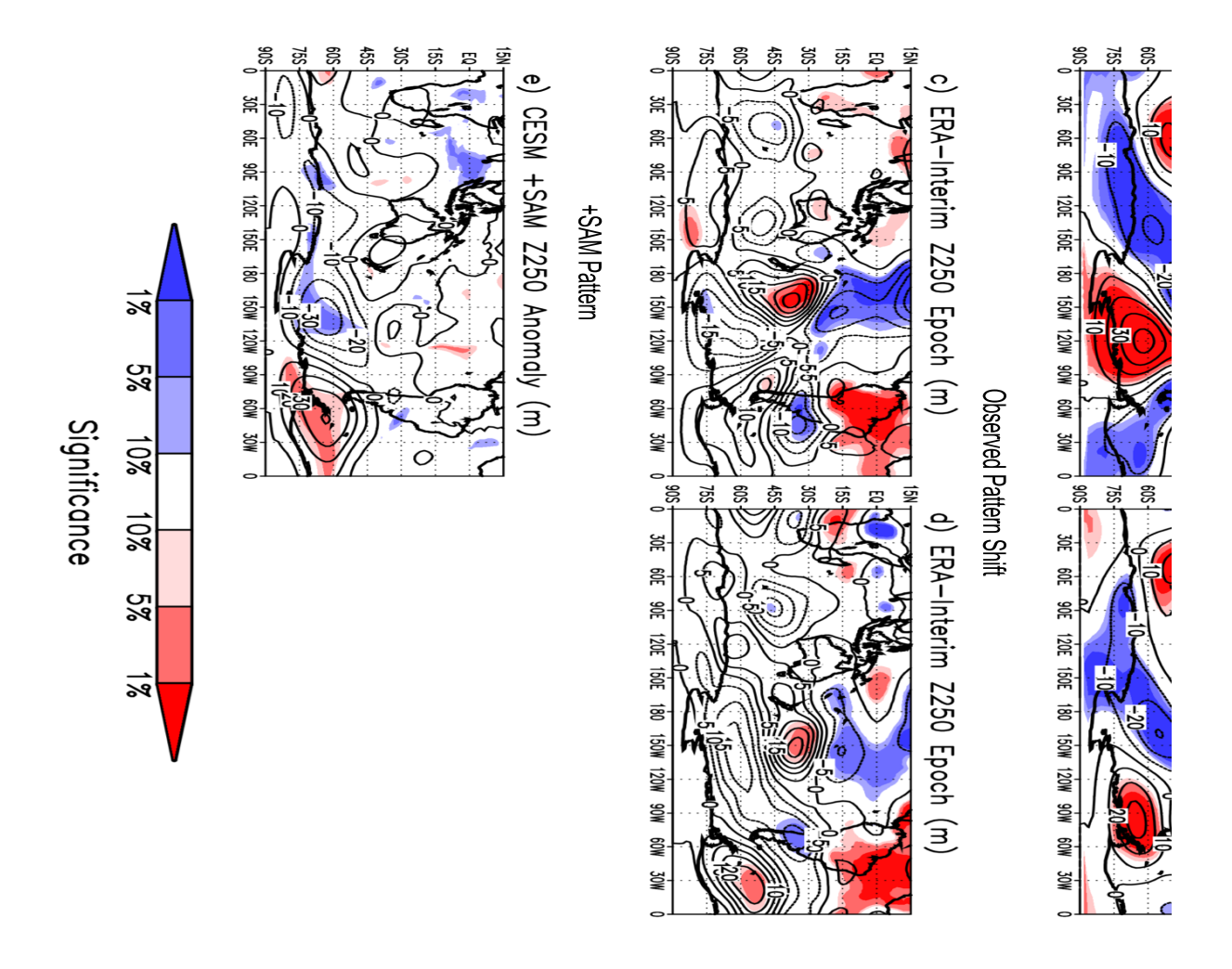


Figure 3. Seasonal circulation and thermal advection anomalies from SPCZ perturbation. The grouped seasonal SPCZ perturbation anomalies (perturbed minus control) of (a,b) Z250 (contours; m) and (c,d) thermal advection at 500 hPa (contours; °C day-1) for austral warm months (DJFMAM; a,c) and cold months (JJASON; b,d). Statistical significance of anomalies is shaded as in Fig. 1.



**Figure 4.** The seasonal signature of the SPCZ teleconnection in observed circulation shifts over 1979-2014. (a-b) The Z250 zonal anomalies (contours, m) for the SPCZ perturbation for (a) DJFMAM and (b) JJASON. (c-d) The epoch difference of ERA-Interim Z250 zonal anomalies (contours, m) shown as the difference between 1999-2014 and 1979-1998 for (c) DJFMAM and (d) JJASON. (e) DJFMAM Z250 zonal anomaly composite anomalies (contour, m) for 4 highest positive SAM index (difference in zonal Z250 at 40°S and 65°S) years in the SPCZ perturbed run compared to the 30-year SPCZ perturbed climatology. The statistical significance of the anomalies is shaded as shown in reference color bar at bottom.